

Carrier distribution in graded-band-gap semiconductors under asymmetric band-edge gradients

S. K. Chattopadhyaya and V. K. Mathur

Department of Physics, Kurukshetra University, Kurukshetra, India

(Received 30 April 1973)

The authors have discussed earlier the photomagnetolectric effect in graded-band-gap semiconductors assuming symmetrical band-edge gradients. The present paper rewrites the continuity equation under asymmetric band-edge gradients, and includes the effects of position-dependent minority carrier lifetime, electron and hole mobilities, and effective masses. A study of excess minority carriers as a function of position in the direction of graded composition indicates that under steady photoexcitation, minority carrier distribution and total concentration of carriers are markedly dependent on the relative magnitudes of conduction- and valence-band-edge gradients. A plausible physical explanation of the carrier distribution in the graded-band-gap specimen has been attempted.

I. INTRODUCTION

The authors¹ have earlier discussed the photomagnetolectric effect in graded-band-gap semiconductors assuming a symmetric funnel-shaped band gap. This, however, is an oversimplified picture, and the recent work of Lauer and Williams² indicates that the conduction-band-edge gradient will, in general, be different from the valence-band-edge gradient in a graded-mixed crystal. It was shown by these authors² that in the case of a graded-mixed specimen in which cation composition is position dependent, the conduction-band-edge gradient is expected to be larger than that of the valence-band-edge gradient. If, however, anion composition is position dependent the valence-band-edge gradient would be large compared to the conduction-band-edge gradient. In certain cases both these gradients may have the same sign, while in other cases their gradients may be opposite to each other. It is, therefore, deemed fit to reexamine the equation of continuity for minority carriers in these semiconductors and obtain results indicating the effects of conduction- and valence-band-edge gradients, explicitly.

In order to write down an equation of continuity that may be valid under the rather general conditions, one has to incorporate into it the position dependence of the effective mass and mobility of minority carriers. Moreover, the absorption coefficient k_1 may also be strongly position dependent. In fact, the authors have recently applied Urbach's rule for the absorption edge³ to discuss a case in which a crystal of graded composition is illuminated by monochromatic radiation transversely, i. e., in a direction perpendicular to its band-edge gradients. It was shown that the position dependence of k_1 alone would give rise to a photodiffusion effect in the direction of graded composition.⁴ However, for the sake of simplicity

the position dependence of k_1 is ignored in the present investigation. This assumption should be reasonable when the energy of the incident radiation is larger than the maximum band gap of the graded material.

To consider the dependence of effective mass and mobility with position in the case of a graded-band-gap semiconductor, it is felt that two forms of variation readily recommend themselves: (i) a slow variation which can be considered linear and (ii) a fast variation which can be taken to be exponential. Recent work of Marfaing and Chevalier⁵ points out the suitability of the latter case at least in a restricted sense. Fortunately, an exponential variation can be easily accommodated in the equation of continuity. Moreover, a linear variation may be deduced from the exponential function as a special case. Therefore, we assume the variation of these quantities as follows:

$$\begin{aligned}\mu_p &= \mu_{p0} e^{b_2 x} , \\ m_p^* &= m_{p0}^* e^{b_3 x} , \\ m_n^* &= m_{n0}^* e^{b_4 x} ,\end{aligned}\quad (1)$$

where μ_p , m_p^* , and m_n^* are the minority-carrier mobility and effective mass, and majority-carrier effective mass, respectively. The subscript 0 denotes the value of respective quantities at $x=0$. The variation with position of the conduction band edge $E_c(x)$ and the valence band edge $E_v(x)$ is taken to be linear:

$$E_c(x) = E_{c0} - \alpha_1 x \quad \text{and} \quad E_v(x) = E_{v0} + \alpha_2 x . \quad (2)$$

Depicted in Fig. 1 are the cases which are later investigated numerically. In Fig. 1(a) the gradients of conduction band edge and valence band edge are opposite to each other and ν , which represents the ratio (α_2/α_1) in the restricted sense discussed in Sec. IV, is negative. In Fig. 1(b) the gradients are of the same sign, and thus ν is positive.

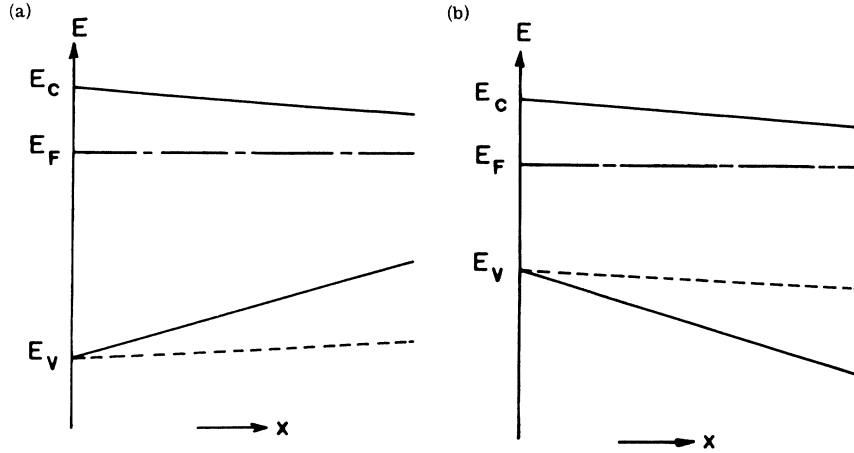


FIG. 1. Asymmetric band-edge gradients (a) $\nu = -4.5$ (continuous line), $\nu = -0.5$ (broken line) conduction-band-edge is common to both; (b) $\nu = +4.5$ (continuous line), $\nu = +0.5$ (broken line) conduction-band-edge is common to both.

It has been shown by Van Ruyven and Williams⁶ that a space-charge-free graded mixed semiconductor crystal can be obtained by inhomogeneous doping. We shall assume here that we are dealing with a graded-band-gap semiconductor which is nondegenerate and strongly n type. In such a case the concentration of minority carriers is influenced by the conduction-band-edge gradient only through the band-to-band radiative recombination lifetime τ_p of the minority carriers. It is, therefore, presumed that in the present case band-to-band radiative transition is the predominant mode of recombination of the excess carriers. Physically such a condition would be significant for semiconductors in which the flaw density is very small. The variation of τ_p with position can be derived as follows.

Band-to-band recombination lifetime τ_p is given by⁷

$$\tau_p \approx n_0 p_0 / G_R (n_0 + p_0 + n_e) \quad (3)$$

where n_0 and p_0 are electron and hole concentrations in thermal equilibrium and n_e is the number of excess carriers. G_R stands for rate of recombination in thermal equilibrium. For an n -type semiconductor under small-signal conditions

$$\tau_p \approx p_0 / G_R \quad (4)$$

Now

$$G_R \propto e^{-(E_C - E_V) / kT} = (\text{const.}) e^{-(E_C - E_V) / kT} \quad (5)$$

and

$$p_0 = (\text{const.}) (m_p^*)^{3/2} e^{(E_V - E_F) / kT} \quad (6)$$

thus

$$\tau_p \approx (\text{const.}) e^{-[(\alpha_1 / kT) - b_3]x} = (\text{const.}) e^{b_1 x} \quad (7)$$

where

$$b_1 = -[(\alpha_1 / kT) - b_3] \quad (7)$$

An attempt was made by Marfaing and Chevallier⁵

to solve such a problem. Their analysis, however, does not take into account the space dependence of volume generation and does not consider the effect of surface states. Furthermore, it does not consider separately the conduction- and the valence-band-edge gradients. In the analysis to follow, an attempt is made to show how the minority-carrier distribution is influenced by the relative magnitude of band-edge gradients.

II. EQUATION OF CONTINUITY

Following Gora and Williams,⁸ the appropriate continuity equation for excess minority-carrier density P can be written as follows:

$$\frac{\partial P}{\partial t} + P \left(\frac{1}{\tau_p} + \mu_p \frac{dF_p}{dx} + F_p \right) + \frac{dP}{dx} \left(\mu_p F_p - \frac{kT}{e} \frac{d\mu_p}{dx} \right) - \frac{kT \mu_p}{e} \frac{d^2 P}{dx^2} = k_1 I e^{-k_1 x} \quad (8)$$

where

$$F_p = E + \frac{1}{e} \left(\frac{dE_v}{dx} + \frac{3kT}{2m_p^*} \frac{dm_p^*}{dx} \right)$$

and I is the intensity of the incident radiation. Using Eq. (1), and in the absence of any external electric field, the equation of continuity (8) under steady-state conditions may be written

$$\frac{d^2 P}{dx^2} - \frac{dP}{dx} \left[\left(\frac{\alpha_2}{kT} + \frac{3b_3}{2} \right) - b_2 \right] - P \left\{ \frac{e}{kT \tau_{p0} \mu_{p0}} \exp \left[-(b_1 + b_2)x + b_2 \left(\frac{\alpha_2}{kT} + \frac{3b_3}{2} \right) \right] \right\} = - \frac{ek_1 I}{kT \mu_{p0}} e^{-(k_1 + b_2)x} \quad (9)$$

By defining $z = e^{-(b_1 + b_2)x} = e^{-bx}$, Eq. (9) may be reduced to standard Bessel form as follows:

$$z^2 \frac{d^2 P}{dz^2} + z \frac{dP}{dz} \left[1 + \frac{1}{b} \left(\frac{\alpha_2}{kT} + \frac{3b_3}{2} - \frac{b_2}{b} \right) \right]$$

$$+P \left[\frac{-ez}{kTb^2\mu_{p0}\tau_{p0}} - \frac{b_2}{b^2} \left(\frac{\alpha_2}{kT} + \frac{3b_3}{2} \right) \right]$$

$$= -\frac{k_1 I_e}{kTb^2\mu_{p0}} z^{(k_1+b_2)/b} \quad (10)$$

The general solution of Eq. (10) is given by⁹

$$P = z^{r/2} [C_1 I_\nu(z') + C_2 I_{-\nu}(z')] = C_1 U_1 + C_2 U_2 \quad (11)$$

where

$$r = \frac{1}{b} \left[b_2 - \left(\frac{\alpha_2}{kT} + \frac{3b_3}{2} \right) \right] \quad ,$$

U_1 and U_2 stand for $z^{r/2} I_\nu(z')$ and $z^{r/2} I_{-\nu}(z')$, respectively, and

$$\nu = 2 \left\{ \frac{1}{4b^2} \left[b_2 - \left(\frac{\alpha_2}{kT} + \frac{3b_3}{2} \right) \right]^2 + \frac{b_2}{b^2} \left(\frac{\alpha_2}{kT} + \frac{3b_3}{2} \right) \right\}^{1/2} \quad ,$$

which is not likely to be an integer. C_1 and C_2 are functions of z' , which is given by

$$z' = \beta z^{1/2}; \quad \beta = (2/b) (e/kT\mu_{p0}\tau_{p0})^{1/2} = 2/bL_{p0} \quad .$$

C_1 and C_2 are given by⁹

$$C_1 = - \int \frac{h(z)U_2}{W[U_1, U_2]} dz + P_1 \quad , \quad (12)$$

$$C_2 = \int \frac{h(z)U_1}{W[U_1, U_2]} dz + P_2 \quad ,$$

where P_1 and P_2 are constants to be determined, and $W[U_1, U_2]$ is the Wronskian, the value of which for a noninteger ν is given by

$$W = U_1 U_2' - U_1' U_2 = -z^{(r-1)} \sin \nu \pi / \pi \quad ,$$

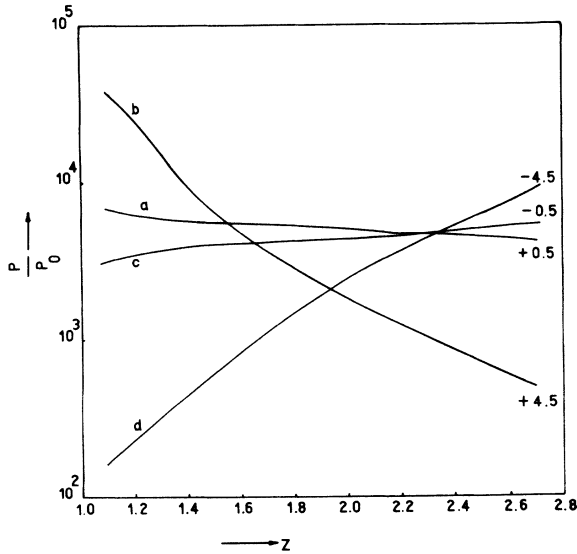


FIG. 2. Carrier distribution with position for small surface recombination ($S_1=10^{-5}$, $S_2=10^{-3}$, $\omega=10^{-4}$ cm, $b\omega=-1$, $K=2k_1/b=-10$). (a) $\nu=+0.5$, (b) $\nu=+4.5$, (c) $\nu=-0.5$, (d) $\nu=-4.5$.

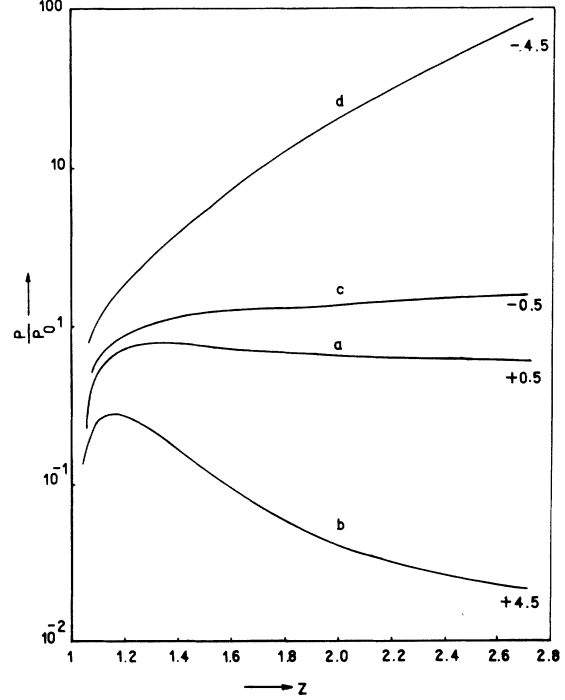


FIG. 3. Carrier distribution with position for large front-surface recombination ($S_1=10^5$, $S_2=10^{-3}$, $K=-10$, $\omega=10^{-4}$ cm, $b\omega=-1$). (a) $\nu=+0.5$, (b) $\nu=+4.5$, (c) $\nu=-0.5$, (d) $\nu=-4.5$.

and

$$h(z) = -\frac{k_1 I_e}{kT\mu_{p0}b^2} z^{(k_1+b_2/2)-2} \quad .$$

Thus the complete solution of P is given by

$$P = \frac{2k_1 I_e \pi \beta^{-(m+1)} z^{r/2}}{kT\mu_{p0}b^2 \sin \nu \pi} [\mathcal{J}(z') + P_1 I_\nu + P_2 I_{-\nu}] \quad , \quad (13)$$

where

$$\mathcal{J}(z') \equiv I_{-\nu} \int z'^m I_\nu dz' - I_\nu \int z'^m I_{-\nu} dz' \quad ;$$

$$m = 2(k_1 + b_2)/b - r - 1 \quad .$$

III. BOUNDARY CONDITIONS

The constants P_1 and P_2 can be evaluated by applying appropriate boundary conditions. To obtain the boundary conditions, one has to deduce an expression for excess minority-carrier diffusion current. Following Cohen-Solal and Marfaing¹⁰ we write for the ambipolar diffusion current

$$i_p = -\frac{\mu_n \mu_p (n_0 + p_0) kT}{(p\mu_p + n\mu_n)} \left[\frac{dP}{dx} + P \left\{ \frac{1}{2kT} \frac{dE_g}{dx} - \frac{3}{4} \frac{d}{dx} (\ln m_p^* m_n^*) \right\} + \frac{P(\delta-1)}{2(\delta+1)} \frac{d}{dx} \ln \delta \right] \quad , \quad (14)$$

where $\delta = n_0/p_0$ is the doping ratio. Now for a

space-charge free graded-band-gap semiconductor, the following relation may be obtained after substituting the usual expressions for n_0 and p_0 ,

$$\frac{d}{dx} \ln \delta = \frac{3}{2}(b_4 - b_3) + \frac{\alpha_1 - \alpha_2}{kT} \quad (15)$$

Furthermore, for a nondegenerate strongly n -type semiconductor (i. e., $n_0 \gg p_0$) and low injection levels, Eq. (14) takes the form

$$i_p = -kT\mu_p \left[\frac{dP}{dx} - P \left(\frac{\alpha_2}{kT} + \frac{3b_3}{2} \right) \right] \quad (16)$$

Thus the boundary conditions at the front ($x=0$) and the back ($x=\omega$) surfaces may be given by the following relations:

$$\begin{aligned} i_p(0) &= -kT\mu_{p0} \left[\frac{dP(0)}{dx} - P(0) \left(\frac{\alpha_2}{kT} + \frac{3b_3}{2} \right) \right] \\ &= -P(0)s_1 e \quad , \end{aligned} \quad (17)$$

$$\begin{aligned} i_p(\omega) &= -kT\mu_{p\omega} \left[\frac{dP(\omega)}{dx} - P(\omega) \left(\frac{\alpha_2}{kT} + \frac{3b_3}{2} \right) \right] \\ &= P(\omega)s_2 e \quad , \end{aligned}$$

where s_1 and s_2 are, respectively, the front- and back-surface recombination velocities. For the sake of convenience, the above equations are re-written

$$\begin{aligned} D_p(0) \frac{dP(0)}{dx} &= P(0) \left[s_1 + D_p(0) \left(\frac{\alpha_2}{kT} + \frac{3b_3}{2} \right) \right] \\ &= P(0)s'_1 \quad , \\ D_p(\omega) \frac{dP(\omega)}{dx} &= -P(\omega) \left[s_2 - D_p(\omega) \left(\frac{\alpha_2}{kT} + \frac{3b_3}{2} \right) \right] \\ &= -P(\omega)s'_2 \quad , \end{aligned} \quad (18)$$

where $D_p(0) = kT\mu_{p0}/e$ and $D_p(\omega) = kT\mu_{p\omega}/e$.

From Eqs. (13) and (18) the constants P_1 and P_2 are obtained as follows:

$$\begin{aligned} P_1 &= \frac{A}{\lambda} \left[\left(\frac{\beta b}{2} \mathcal{J}'_0 + \frac{rb}{2} \mathcal{J}_0 + \frac{s'_1}{D_p(0)} \mathcal{J}_0 \right) \left(\frac{bz'(\omega)}{2} I_{-\nu\omega} + \frac{rb}{2} I_{-\nu\omega} - \frac{s'_2}{D_p(\omega)} I_{-\nu\omega} \right) - \left(\frac{\beta b}{2} I'_{-\nu 0} + \frac{rb}{2} I_{-\nu 0} + \frac{s'_1}{D_p(0)} I_{-\nu 0} \right) \right. \\ &\quad \left. \times \left(\frac{bz'(\omega)}{2} \mathcal{J}'_\omega + \frac{rb}{2} \mathcal{J}_\omega - \frac{s'_2}{D_p(\omega)} \mathcal{J}_\omega \right) \right] \quad , \\ P_2 &= \frac{A}{\lambda} \left[\left(\frac{\beta b}{2} I'_{\nu 0} + \frac{rb}{2} I_{\nu 0} + \frac{s'_1}{D_p(0)} I_{\nu 0} \right) \left(\frac{bz'(\omega)}{2} \mathcal{J}'_\omega + \frac{rb}{2} \mathcal{J}_\omega - \frac{s'_2}{D_p(\omega)} \mathcal{J}_\omega \right) - \left(\frac{bz'(\omega)}{2} I'_{\nu\omega} + \frac{rb}{2} I_{\nu\omega} - \frac{s'_2}{D_p(\omega)} I_{\nu\omega} \right) \right. \\ &\quad \left. \times \left(\frac{\beta b}{2} \mathcal{J}'_0 + \frac{rb}{2} \mathcal{J}_0 + \frac{s'_1}{D_p(0)} \mathcal{J}_0 \right) \right] \quad , \end{aligned} \quad (19)$$

where $A = 2k_1 I e \pi \beta^{-(m+1)} / kT \mu_{p0} b^2 \sin \nu \pi$, and

$$\begin{aligned} \lambda &= \left(\frac{\beta b}{2} I'_{-\nu 0} + \frac{rb}{2} I_{-\nu 0} + \frac{s'_1}{D_p(0)} I_{-\nu 0} \right) \left(\frac{bz'(\omega)}{2} I'_{\nu\omega} + \frac{rb}{2} I_{\nu\omega} - \frac{s'_2}{D_p(\omega)} I_{\nu\omega} \right) - \left(\frac{\beta b}{2} I'_{\nu 0} + \frac{rb}{2} I_{\nu 0} + \frac{s'_1}{D_p(0)} I_{\nu 0} \right) \\ &\quad \times \left(\frac{bz'(\omega)}{2} I'_{-\nu\omega} + \frac{rb}{2} I_{-\nu\omega} - \frac{s'_2}{D_p(\omega)} I_{-\nu\omega} \right) \quad . \end{aligned}$$

The subscripts 0 and ω represent the values of the relevant quantities at $x=0$ and $x=\omega$. \mathcal{J}' and I' represent the derivatives of \mathcal{J} and I with respect to z' .

IV. RESULTS

To understand the role of band-edge gradients we assume α_1/kT , $\alpha_2/kT \gg b_2$, b_3 , b_4 . The position dependence of minority carrier lifetime τ_p under the above conditions may be obtained from Eq. (5). Thus we find,

$$\nu \approx (1/b) \alpha_2/kT \approx -\alpha_2/\alpha_1 \quad , \quad (20)$$

and

$$r \approx \alpha_2/\alpha_1 \quad . \quad (21)$$

To compare P at different values of x from Eqs. (13) and (19) is not easy, first because it is not possible to evaluate exactly the integral $\mathcal{J}(z')$ in an

analytical manner, and, second, because the task of computing P is further complicated, because the values of Bessel function for arbitrary noninteger values of ν are not tabulated. We therefore choose two cases of practical importance in the literature. Cohen-Solal and Marfaing¹⁰ prepared thin films of graded structure for which $|b| \sim 10^4/\text{cm}$. For a film thickness $\omega \sim 10^{-4}$ cm, the magnitude of z' will normally be limited to values below unity. On the other hand, in the work of Williams *et al.*¹¹ $|b| \sim 10/\text{cm}$, for which the magnitude of z' will generally be much greater than one. Under these conditions it is possible to approximate the Bessel functions by the leading terms in their series expansions. These approximations are as follows:

for $|z'| \ll 1$,

$$I_\nu(z') \sim \frac{1}{2^\nu \nu!} z'^\nu ; \quad I_{-\nu}(z') \sim \frac{1}{2^{-\nu} (-\nu)!} z'^{-\nu} \quad ; \quad (22a)$$

for $|z'| \gg 1$,

$$I_\nu(z') \sim \frac{e^{z'}}{(2\pi z')^{1/2}}; \quad I_{-\nu}(z') \sim \left(\frac{\pi}{2z'}\right)^{1/2} e^{-z'}. \quad (22b)$$

(i) For $|z'| \gg 1$, a complete analysis is not possible. However as $I_\nu(z')$ and $I_{-\nu}(z')$ both become independent of ν , it may be remarked that the minority-carrier distribution will be weakly depen-

dent on band-edge gradients.

(ii) For $|z'| \ll 1$, $\mathcal{J}(z')$ can be written with the help of approximations (22a) as

$$\mathcal{J}(z') = \frac{(-2\nu)z'^{m+1}}{\Gamma(\nu+1)\Gamma(-\nu+1)(m+\nu+1)(m-\nu+1)}. \quad (23)$$

P_1 and P_2 may also be approximated to the following forms:

$$P_1 = \frac{A}{\lambda_1} \left[\mathcal{J}_0 I_{-\nu\omega} \left(\frac{b\omega(m+1)}{2} + \frac{rb\omega}{2} + S_1 \right) \left(-\frac{b\omega\nu}{2} + \frac{rb\omega}{2} - S_2 \right) - I_{-\nu\omega} \mathcal{J}_\omega \left(-\frac{b\omega\nu}{2} + \frac{rb\omega}{2} + S_1 \right) \left(\frac{b\omega(m+1)}{2} + \frac{rb\omega}{2} - S_2 \right) \right], \quad (24)$$

$$P_2 = \frac{A}{\lambda_1} \left[I_{\nu\omega} \mathcal{J}_\omega \left(\frac{b\omega\nu}{2} + \frac{rb\omega}{2} + S_1 \right) \left(\frac{b\omega(m+1)}{2} + \frac{rb\omega}{2} - S_2 \right) - I_{\nu\omega} \mathcal{J}_0 \left(\frac{b\omega\nu}{2} + \frac{rb\omega}{2} - S_2 \right) \left(\frac{b\omega(m+1)}{2} + \frac{rb\omega}{2} + S_1 \right) \right],$$

where

$$\lambda_1 = I_{-\nu\omega} I_{\nu\omega} \left(-\frac{b\omega\nu}{2} + \frac{rb\omega}{2} + S_1 \right) \left(\frac{b\omega\nu}{2} + \frac{rb\omega}{2} - S_2 \right) - I_{\nu\omega} I_{-\nu\omega} \left(\frac{b\omega\nu}{2} + \frac{rb\omega}{2} + S_1 \right) \left(-\frac{b\omega\nu}{2} + \frac{rb\omega}{2} - S_2 \right)$$

and $S_1 = s'_1 \omega / D_p(0)$; $S_2 = s'_2 \omega / D_p(\omega)$.

Values of the excess minority-carrier density P may now be plotted as a function of z for values of ν , both positive and negative, using Eqs. (13), (23), and (24). Figures 2-4 give these values for different surface conditions of the graded-band-gap structure.

The effect of ν on the total carrier concentration can be evaluated by considering the photoconductivity G which, according to DeVore,¹² is given by

$$G = \int_0^\omega P dx. \quad (25)$$

Substituting for P from Eqs. (13), (23), and (24), we have:

$$G = \frac{A}{b} \left(\frac{(2\nu)(2\beta^{m+1})(e^{-b\omega(m+1-\nu)/2} - 1)}{\Gamma(-\nu+1)\Gamma(\nu+1)(m+\nu+1)(m-\nu+1)} + P_1 \frac{\beta^\nu b \omega}{2^\nu \Gamma(\nu+1)} + P_2 \frac{2^\nu \beta^{-\nu}}{\nu \Gamma(\nu+1)} (e^{b\omega\nu} - 1) \right). \quad (26)$$

A plot of G for different values of ν is shown in Fig. 5.

V. DISCUSSION

A study of the band-gap variation for the various values of ν depicted in Fig. 1 is the basis for a plausible physical explanation for the minority-carrier distribution shown in Figs. 2-4. We have chosen to consider only positive α_1 , so that b is negative in all our examples. One can analyze the cases for negative values of α_1 and positive b , also along similar lines. However, the present discussion does not include these cases, as they are not expected to give results significantly different from the ones discussed below. Figure 2 corresponds to negligible recombination at both surfaces, so that the variation in P in the specimen is mainly determined by the magnitudes of the

band-edge gradients. Normally one expects that the concentration of the carriers should decrease as one moves away from the illuminated surface to the dark surface. But for large and negative values of ν (assuming positive α_1), the excess carriers generated at the front surface are subjected to a large value of so-called "quasifield" (a term Kroemer¹³ has used to describe the effect of band-edge gradients), which results in their motion away from the front surface. For ν positive and large, the diffusion of carriers which might have resulted in the case of a homogeneous semiconductor due to nonuniform generation in the bulk is hindered by the "quasifield" set up in the opposite direction by the valence-band-edge gradient. Furthermore, owing to small surface recombination, the over-all concentration of carriers in this case, for all values of ν is very large as compared to the cases discussed later, where either front- or back-surface recombination is high.

In Fig. 3 is plotted a case of practical importance, where the front-surface recombination is very large. Note that for ν negative and large, excess minority-carrier diffusion is assisted by the valence-band-edge gradient. The equilibrium concentration therefore increases with position. For positive ν , carrier diffusion is opposed by the valence-band-edge gradient, which increases the probability that carriers will be lost due to recombination at the front surface. In fact, at the front-surface carrier concentration approaches zero because of the very large value of S_1 assumed in this case. Thus after an initial increase P decreases with x , owing to lesser carrier generation and because the valence-band-edge gradient opposes diffusion of carriers towards the dark sur-

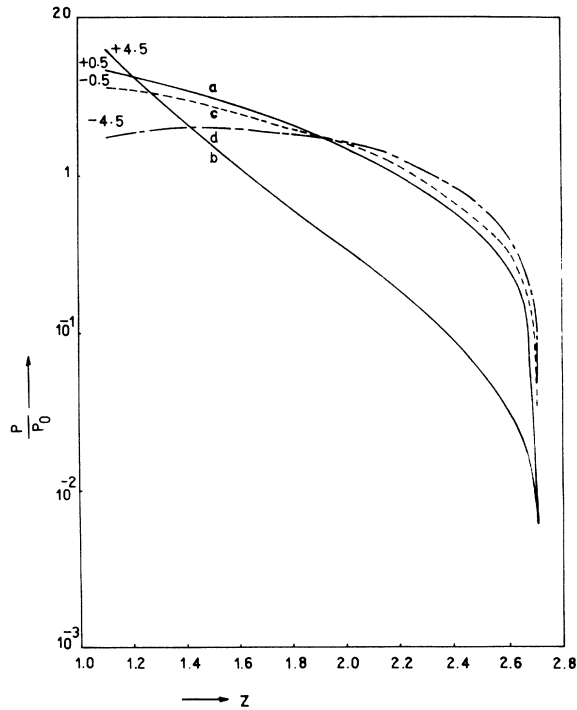


FIG. 4. Carrier distribution with position for large back-surface recombination ($S_1=10^{-3}$, $S_2=10^5$, $K=-10$, $\omega=10^{-4}$ cm, $b\omega=-1$). (a) $\nu=+0.5$, (b) $\nu=+4.5$, (c) $\nu=-0.5$, (d) $\nu=-4.5$.

face. This particular distribution indicates a strong possibility of observing sign reversal in the photodiffusion voltage across the specimen.¹⁴

Figure 4 is a plot of the carrier distribution when back surface recombination is very large. Therefore, for all positive as well as small negative values of ν , the excess minority-carrier concentration decreases with x , with a gradient depending on the magnitude of ν . However, when $\nu=-4.5$ (i.e., large and negative), there is a slight increase in the concentration due to dominant effect of the valence band-edge gradient at small depths below the front surface. But near the back surface, due to high back-surface recombination, the concentration of the minority carriers falls sharply.

In Fig. 5, G has been plotted as a function of ν for the case of large front-surface recombination. These curves show how the total excess minority-carrier concentration would vary with the asymmetry in the band-edge gradients. One finds that for ν large and negative, the photoconductivity is large as the valence-band-edge gradient assists the diffusion of minority carriers away from the front surface where recombination is high. The decrease in photoconductivity with increase in the values of absorption coefficient as seen in Fig. 5 can be explained on the basis of similar results

observed for homogeneous semiconductors.¹² With a larger absorption coefficient, a greater proportion of carriers are created at the front surface where recombination is large.

When ν is positive and large, the case of large back-surface recombination is characterized by a very steep gradient of excess minority carriers (Fig. 4). Thus when the front surface of such a specimen is irradiated, due to the large concentration gradient, both electron and hole pairs generated at the front surface would tend to diffuse to the back surface. However, due to the differential mobility of holes and electrons, a potential difference is developed between the dark and the illuminated surface. Assuming the mobility of holes to be less than that of electrons, the holes lag behind during diffusion and the illuminated surface becomes positive with respect to the dark surface. (In the case of semiconductors for which hole mobilities are higher than those of electrons the illuminated surface will be negative with respect to the dark surface). Furthermore, in the typical situation characterized by Fig. 1(b), the diffusion of electrons to the back surface is assisted by the conduction-band-edge gradient, while the diffusion of holes to the back surface is hindered by the valence-band-edge gradient. Thus the effect achieved by

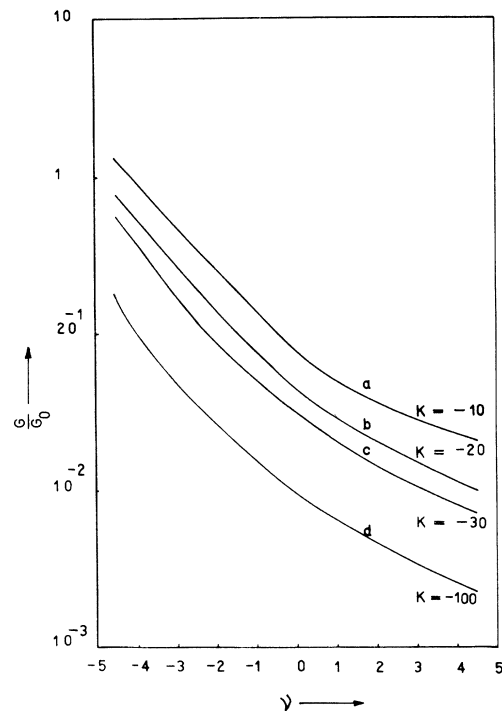


FIG. 5. Variation of photoconductivity with ν for large front-surface recombination ($S_1=10^5$, $S_2=10^{-3}$, $\omega=10^{-4}$ cm, $b\omega=-1$). (a) $K=-10$, (b) $K=-20$, (c) $K=-30$, (d) $K=-100$.

differential mobility is enhanced. This situation may therefore be quite favorable for producing photovoltaages of the Dember type.

ACKNOWLEDGMENT

The authors wish to thank Professor N. Nath for his keen interest and encouragement during the work.

¹S. K. Chattopadhyaya and V. K. Mathur, Phys. Rev. B 3, 3390 (1971).

²R. B. Lauer and F. Williams, J. Appl. Phys. 42, 2904 (1971).

³F. Urbach, Phys. Rev. 92, 1324 (1953).

⁴V. K. Mathur and S. K. Chattopadhyaya, Indo-Soviet Conference on Solid State Materials, 1972, Bangalore (unpublished).

⁵Y. Marfaing and J. Chevallier, Trans. IEEE ED-18, 465 (1971).

⁶L. J. Van Ruyven and F. Williams, Am. J. Phys. 35, 705 (1967).

⁷J. S. Blakemore, *Semiconductor Statistics* (Pergamon,

Oxford, England, 1962), Chap. IV.

⁸T. Gora and F. Williams, Phys. Rev. 177, 1179 (1969).

⁹F. B. Hildebrand, *Advanced Calculus for Applications* (Prentice-Hall, Englewood Cliffs, N. J., 1962), Chaps. I and IV.

¹⁰G. Cohen-Solal and Y. Marfaing, Solid State Electron. 11, 1131 (1968).

¹¹Indradev, L. J. Van Ruyven, and F. Williams, J. Appl. Phys. 39, 3344 (1968).

¹²H. B. Devore, Phys. Rev. 102, 86 (1956).

¹³H. Kroemer, RCA Rev. 18, 332 (1957).

¹⁴W. W. Gärtner, Phys. Rev. 105, 823 (1957).